A Chiral, Low-Cytotoxic [Ni$_{15}$]-Wheel Complex

Simon Muche,[†] Irina Levacheva,[‡] Olga Samsonova,[‡] Linh Pham,[§] George Christou,[§] Udo Bakowsky,[‡] and Małgorzata Hołyńska*,[†,§]

[†]Fachbereich Chemie and Wissenschaftliches Zentrum für Materialwissenschaften (WZMW), Philipps-Universität Marburg, Hans-Meerwein-Straße, D-35032 Marburg, Germany

[‡]Institut für Pharmazeutische Technologie & Biopharmazie, Philipps-Universität Marburg, Ketzerbach 63, D-35032 Marburg, Germany

[§]Department of Chemistry, University of Florida, Gainesville, Florida 32611-7200, United States

S *Supporting Information*

ABSTRACT: A new chiral [Ni$_{15}$] complex with a Schiff-base ligand derived from *o*-vanillin and L-glutamic acid is presented, emphasizing the properties relevant for biology and materials science. The formation of the complex molecules in solution is confirmed by AFM and dynamic light scattering studies. The compound is weakly antiferromagnetic with considerable admixture of excited states, comprising negligibly interacting [Ni$_3$] units. Studies of the interactions with two cell lines indicate low cytotoxicity.
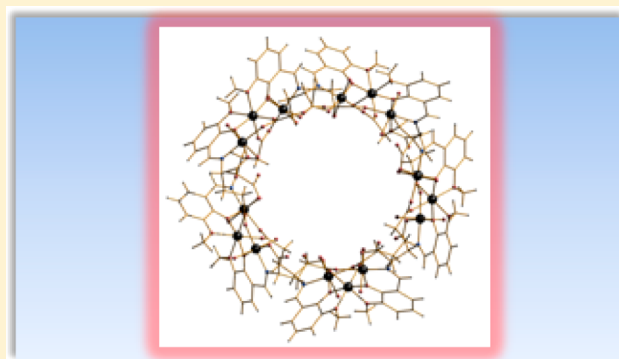
1. INTRODUCTION

Polynuclear metal complexes are of high importance in bioinorganic chemistry, yet their biological activity is scarcely explored due to the complexity of these systems and is limited mainly to Pt/Ru compounds.[1] In particular, simple complexes with Schiff-base ligands are known to often display antibacterial activity[2] and to act as models for enzymes.[3] At the same time, they often serve as magnetic materials, showing single-molecule magnet behavior.[4] Beside a wide variety of physical applications the wheel-like structures can play a significant role in many biochemical processes, such as micelle formation[5−8] and insertion of proteins into biological membranes.[9] It is assumed that large wheel-shaped molecules can be potentially used for DNA binding, due to the negative charge present on their surface.[10] Recent research focuses not only on antitumor activity of, for example, Pt(II) compounds, but also on introducing low-cytotoxic drug nanocarriers based on metal complexes.[1c] These compounds may play the role of "Trojan horses", delivering cytotoxic species into target tissue.[1c]

In this paper we report on the synthesis and properties of a chiral high-nuclearity [Ni$^{II}_{15}$] complex (**1**), incorporating a Schiff-base ligand derived from a natural amino acid. The compound is a rare example of an odd-number wheel-like Ni(II) cluster. Concomitantly the related compound was synthesized by Vittal et al.[11a] by a different method. The known even-numbered Ni(II) wheel-like molecules include the highest nuclearity [Ni$_{24}$] assemblies. Winpenny et al.[11b] contributed an [Ni$_{24}$] complex with a heterocyclic 3-methyl-3-pyrazolin-5-one ligand.[11b] Recently also an [Ni$_{24}$] wheel-like complex with isophthalate as a ligand, forming a 3D coordination polymer, has been reported by Tao et al.[11c] An [Ni$_{20}$L$_4$(HL)$_4$(OAc)$_{28}$] (H$_2$L = 3-[benzyl(2-hydroxyethyl)-amino]-1-propanol) complex with a central [Ni$_{12}$] loop and four peripheral [Ni$_2$] fragments is also known.[11d] Other nuclearity Ni(II) wheels include [Ni$_{16}$],[11e] [Ni$_{12}$],[11f−i] [Ni$_{11}$],[11j] [Ni$_{10}$],[11k] and [Ni$_6$][11l,m] compounds. On the other hand, the [Ni$_{15}$] complexes displaying different topologies include a selenium-bridged [Ni$_{15}$Se$_{15}$(PPh$_3$)$_6$] cluster reported by Fenske and Ohmer,[12a] displaying a barrel-like structure. A sulfur-bridged analogue was introduced by Liu et al.,[12b] whereas a similar complex with a different phosphine ligand was synthesized by Midollini et al.[12c] Albano et al.[12d] synthesized an antimony-bridged nickel(II) carbonyl cluster, [NEt$_3$CH$_2$Ph]$_2$[Ni$_{15}$(μ_{12}-Sb)(CO)$_{24}$], with a distorted Sb-centered [Ni$_{12}$(μ_{12}-Sb)] icosahedral moiety capped with three Ni atoms.
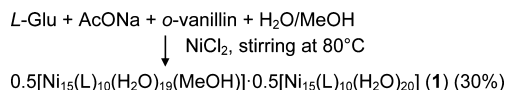
2. RESULTS AND DISCUSSION

2.1. Syntheses and Structure. The Schiff-base ligand, being a constituent of the title complex, is formed *in situ* in the reaction of *o*-vanillin and L-glutamic acid in the presence of sodium acetate (Scheme 1).

The ligand has been already mentioned in physicochemical studies on its metal complexes, however, with no crystal structure determinations.[13] The known reports on the metal

## Scheme 1. Overview of the Procedure for Isolation of 1[a]

L-Glu + AcONa + o-vanillin + H$_2$O/MeOH

↓ NiCl$_2$, stirring at 80°C

0.5[Ni$_{15}$(L)$_{10}$(H$_2$O)$_{19}$(MeOH)]·0.5[Ni$_{15}$(L)$_{10}$(H$_2$O)$_{20}$] (**1**) (30%)

[a]L-Glu = L-glutamic acid, H$_3$L = the Schiff-base ligand.

ion complexation include mainly spectroscopic, polarographic, potentiometric, or molecular modeling studies. An example is the report on polarographic behavior of chromium(III) complexes published by Malik et al.[13b] Our attempts to isolate the ligand in crystalline form have so far been unsuccessful. On the other hand, formation of an oily product can be confirmed. The title complex is an [Ni$_{15}$] neutral chiral assembly with 10 bridging ligands, being a Schiff base derived from o-vanillin and L-glutamic acid. The Schiff-base ligand adopts the coordination mode illustrated in Scheme 2. The two carboxylate groups are mono/bidentately coordinated with *anti/syn−syn* mode (Scheme 2).

Scheme 2. Coordination Mode of the Schiff-Base Ligand in 1
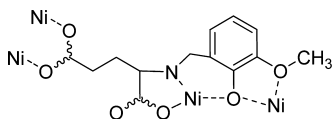
The oxidation state of the Ni^{2+} ions is confirmed by charge balance considerations and studies of the magnetic properties. Due to extensive disorder of the organic part/solvent in the crystal structure, only a limited discussion of the molecule's geometrical parameters is possible. The wheel-like assembly is of 11/24 Å of inner/outer diameter, respectively (Figure 1, top). In the complex molecule trinuclear [Ni$_3$] units with Ni^{2+} ions at closest distances can be distinguished (at 3.42(1)− 3.462(2) Å; see Table S3). Schematic structure of one of the [Ni$_3$] units is presented in Figure 1 (bottom). The Ni^{2+} ion arrangement is linear, which suggests two equivalent pathways for magnetic interactions. A similar construction basis was observed by Winpenny et al.[11a] for their [Ni$_{24}$] wheel-like complexes with a 3-methyl-3-pyrazolin-5-one ligand. In each [Ni$_3$] unit in **1** two Ni^{2+} ions are linked by a double oxo-acetato bridge. The oxo part is the ligand o-vanillin part phenoxo atom; the acetate comes from the L-glutamic acid carboxylate group bonded to γ-C and coordinates in a *syn, syn* mode. Thus, two perpendicular rings are defined, joined by one Ni^{2+} ion. Each ring is slightly puckered with Ni−O−C−O torsion angles of, for example, 21(2)°, 26(2)° and 21(2)°, 25(2)° for the Ni1− Ni2 and the Ni2−Ni3 ring, respectively. The representative bond angles are highlighted in Figure 1 (bottom). Each thus defined unit is at ~8.3−9.3 Å from the equivalent unit, magnetically isolated with the organic ligands. Each Ni^{2+} ion displays a distorted octahedral coordination environment. The central Ni^{2+} ion of each [Ni$_3$] unit is surrounded solely by ligand O atoms. Four ligands are participating in this arrangement: two ligands are chelating through one methoxo and one phenoxo O atom; the other two ligands donate one acetate O atom each. The other two Ni^{2+} ions of the [Ni$_3$] unit display coordination environments analogous to each other. Thus, in both cases two water ligands are coordinated to the central metal atom in a *trans* arrangement, where one ligand points outside and the second ligand points inside the molecule. The water ligand pointing inside should be involved
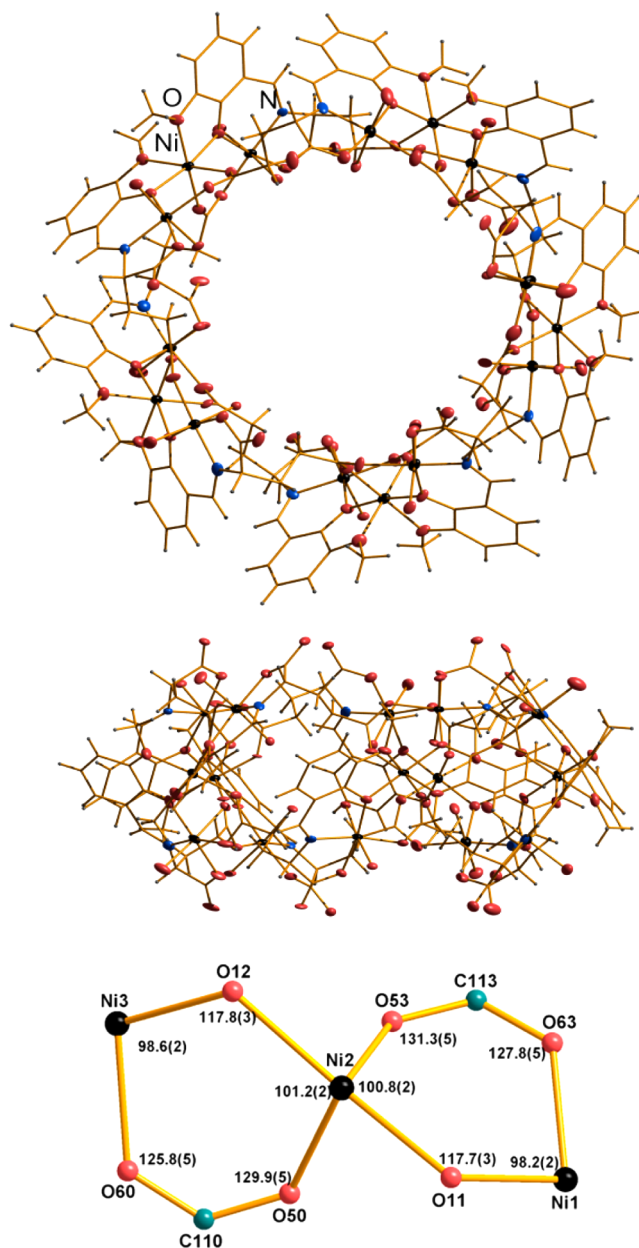
Figure 1. Molecular structure of the title complex (top), along with the side view (middle) and schematic structure of one of the [Ni$_3$] units (bottom). Disordered part is omitted for clarity. Thermal ellipsoids of non-C/H atoms are plotted at the 20% probability level.

in intramolecular hydrogen bonds to the acetate O atoms available as acceptors. The coordination spheres are completed by two organic ligands: one donates a single acetate O atom; the second ligand chelates through phenoxo/methoxo O atoms and one N atom.

The complex molecules in the crystal structure form overlapping columns extending along [100] (Figure 2) with heavily disordered solvent molecules inside and outside the columns. A network of hydrogen bonding is present, which is difficult to describe in detail due to extensive disorder.

2.2. AFM Study. The high solubility of **1** in methanol can be utilized to prepare the AFM slides. In order to prepare a monolayer of the examined substance, the solution in methanol was deposited on a silicon wafer. The AFM studies (Figure 3) revealed two major types of structures: small rounded point-
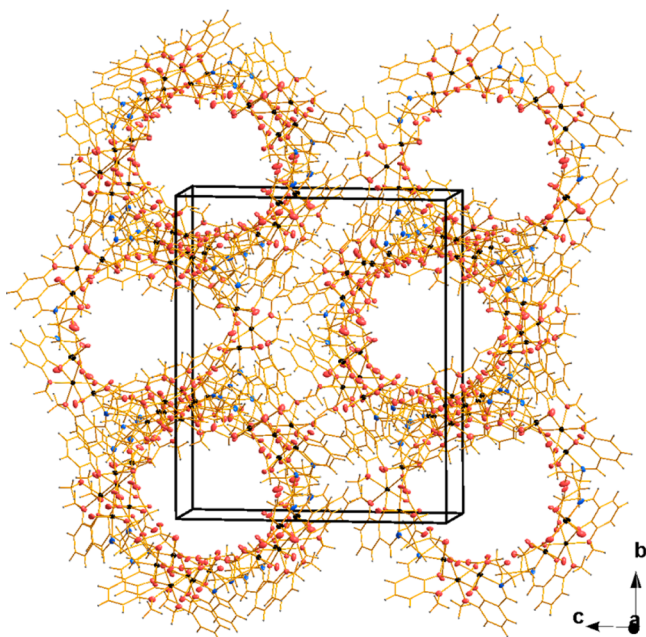
Figure 2. Packing of the complex molecules in **1**. Solvent molecules are omitted for clarity.
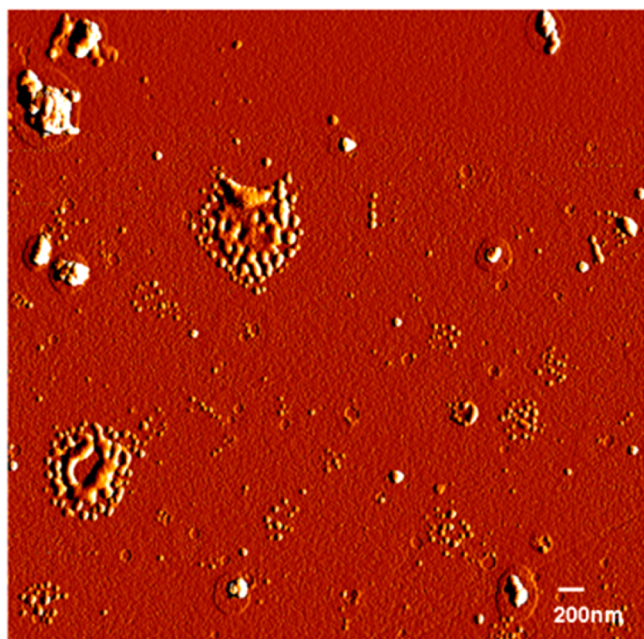

Figure 3. AFM image on deposition from the solution of **1** in methanol.

shaped structures under 10 nm size, which are assumed to be the molecules of **1**, along with larger round and irregular assemblies of 100−500 nm diameter assumed to be agglomerates of the complex molecules.

2.3. Dynamic Light Scattering Study. Studies of a 95% water/5% methanol solution of **1** were undertaken by dynamic light scattering (Figure S3). Interestingly, the obtained data correlate well with the AFM results for a solution in methanol. In both cases an aggregation is observed, most probably due to noncovalent interactions (see SI). Thus, larger aggregates of several hundred nanometer diameters can still be observed, along with a ~2.7 nm size component corresponding to the

complex molecules **1**. Simple IR studies for residues left upon evaporating the solutions support this conclusion (see SI). The peak assignable to species under 0.5 nm in size might indicate partial hydrolysis of the molecular wheels.

2.4. Cytotoxicity Study. The solution studied by dynamic light scattering (5% methanol/95% water) was examined for interaction with two cellular lines in order to assess the potential toxicity of **1**. The following cell lines were used: L929, subcutaneous connective mouse tissue; areolar and adipose, adherent cell line with fibroblast morphology (L929 is used by United States Pharmacopoeia for biocompatibility tests); B16, skin tissue, mouse melanoma, mixture of spindle-shaped and epithelial-like cells, adherent cell line (a fast growing cell line with intensive metabolism). With both *in vitro* assays (MTT and LDH) no IC_{50} (50% cellular toxicity) value could be reached in the tested concentration range. This means that **1** does not demonstrate any pronounced acute and long-term necrotic or apoptotic activity upon contact with the living cells in the given exposure time. Low-range inhibition of metabolism observed for L929 and B16 cell lines (Figures 4 and 5) cannot be assigned to a selective substance effect.
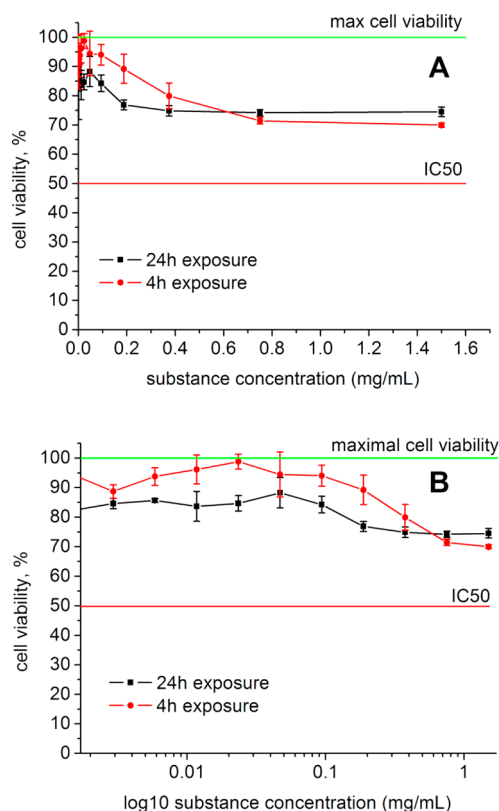

Figure 4. Mitochondrial activity of mouse melanoma with different exposure to the test substance **1**: (A) direct concentration dependence, (B) logarithmic dependence, which is used for the IC_{50} calculation.

It is interesting to note that the melanoma cells have a slightly more pronounced metabolism drop in a lower concentration range, which may be due to a faster accumulation in the cells, as these cells have a faster doubling time.[14] The difference in interactions with malignant and normal cells may be better distinguished at higher concentration ranges. For both cell lines the long-term exposure (24 h) had more impact on the cell metabolism, which is common for non-physiological substances and their accumulation in the tissue.[15]
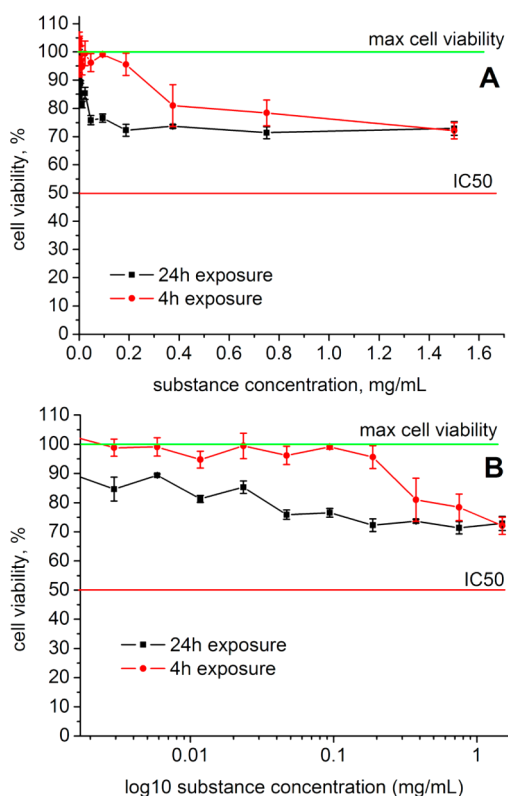
Figure 5. Mitochondrial activity of mouse fibroblasts with different exposure to the test substance **1**: (A) direct concentration dependence, (B) logarithmic dependence, which is used for IC$_{50}$ calculation.

The LDH assay matches the results obtained for the MTT assay in the short- and long-term toxicity trend (Figure 6). The 24 h incubation with **1** leads to a stronger LDH-level expression for both cell lines, as expected. This was observed due to accumulation of the metabolites in the cell culture wells. Each cell line can reach up to 10% cellular toxicity under physiological conditions due to accumulation of the cell metabolism products over a longer exposure time. A toxic control with Triton-X led to complete cell lysis and developed 100% LDH toxicity. Our results allow us to define the analyzed substance as a promising agent of low cytotoxicity, as it does not reach the IC$_{50}$ in both short- and long-term exposure times. On the other hand, both simple Ni(II) salts, such as acetate or chloride, and complex compounds, such as $[NEt_4]_2[NiCl_4]$, are cytotoxic already at concentrations of 100 μM (please see refs 16−27 and those for the compounds mentioned below). The majority of the studied complexes are mononuclear. Especially

high cytotoxicity is displayed by mononuclear Ni(II) semi-carbazone/thiosemicarbazone-functionalized chinone derivatives as ligands.[17] The analogous Pd/Cu complexes are weakly cytotoxic. Binuclear $[Ni_2]$ complexes with 3,3-dialkyl/aryl-1-benzoylthiourea as a ligand are cytotoxic toward T47D cell lines and have a higher effect than "cisplatin".[27] Polynuclear (tri- to pentanuclear) Ni(II) complexes derived from salicylhydroxamic acid interact with DNA and show antibacterial activity.[28] An interesting example is an $[Ni_4]$ complex with a biphenol-based ligand, inducing condensation of DNA, but no cleavage and no cytotoxicity.[29]

2.5. Magnetic Properties. $\chi_M T$ vs T curves recorded for **1** (Figure 7a) show dominating antiferromagnetic behavior (Figure 8, Weiss constant of −2.4 K in the linear region). The $\chi_M T$ value at room temperature is about 13.58 cm^3 K/mol, which is smaller than expected for 15 non-interacting Ni^{2+} ions ($S = 1$, 15.00 cm^3 K/mol). The decrease at low temperatures may be a combined effect of weak antiferromagnetic interactions and zero field splitting effects. The drop in the in-phase ac $\chi_M'T$ values at lower temperatures (Figure 9) suggests that the spin ground state is not well isolated, and the excited states are populated even at low temperatures, probably due to the weak magnetic interactions within the system. As a consequence, it was also not possible to provide a reasonable fit of the reduced magnetization data (Figure 10). The presence of low-lying excited states was also reported for the carboxylate-bridged $[Ni_{12}]$ complexes comprising three tetranuclear units stabilized by a central templating anion in a wheel-like arrangement.[30]

The complex molecules in **1** contain five $[Ni_3]$ units linked through carboxylate−phenoxido bridges. The units are essentially magnetically isolated by the organic ligand parts. Thus, for the first approximation, the fit of the magnetic data was based on a simple trinuclear model (Scheme 3) under the assumption that the trinuclear units do not interact. In this model the J' constant value (Scheme 3) is expected to be very low. The corresponding van Vleck equation is quoted in the SI.

For nickel(II) complexes the g values should be greater than 2.0, as expected for d^6−d^9 metals. On the basis of the reported exchange coupling parameters between two Ni^{2+} ions bridged by carboxylate and/or phenoxido ligands,[31] the J value is expected to be small, but still should remain higher than J'. Thus, constraints of $g > 2$ and also of $J < 10$, along with $J' > -10$, were applied. The TIP value was kept at 6.0×10^{-4} cm^3 mol^{-1}. Moreover, because of the weak coupling between the Ni centers, the effect of intermolecular interactions becomes more significant and cannot be ignored at very low temperatures.
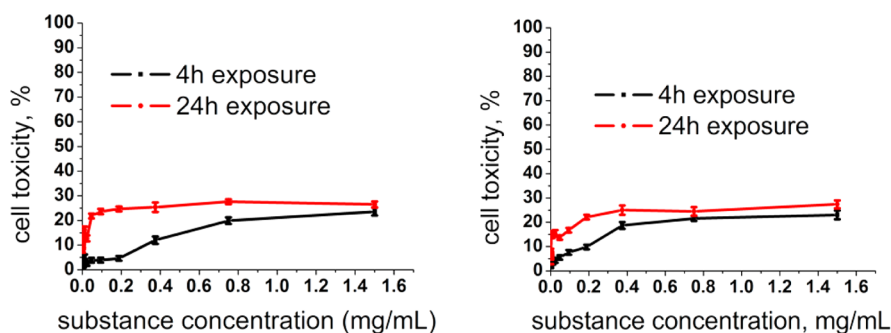

Figure 6. LDH cellular toxicity in mouse fibroblasts (left) and mouse melanoma (right) with different exposure times to the test substance **1**.
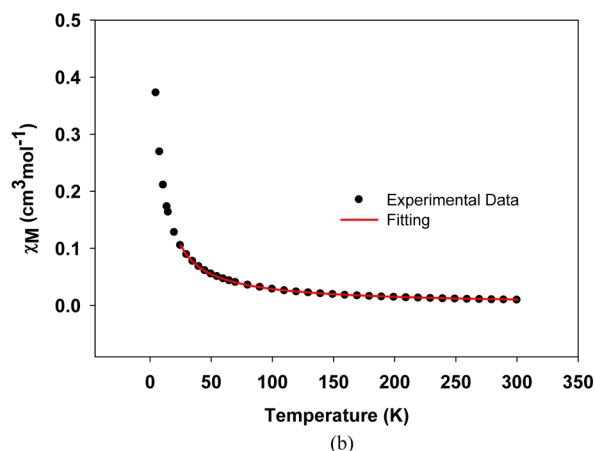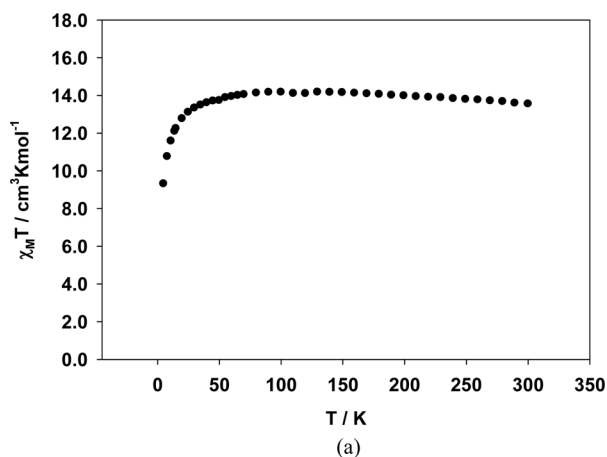
Figure 7. Plot of the (a) $\chi_M T$ vs T and (b) χ_M vs T dependence for **1** in a 0.1 T field (the solid line shows a fit to the corresponding van Vleck equation with the resulting parameters $J = -4.4(8)$, $J' = -0.3(4)$ cm^{-1}, $g = 2.00(5)$; goodness of fit coefficient $R^2 = 0.9992$).
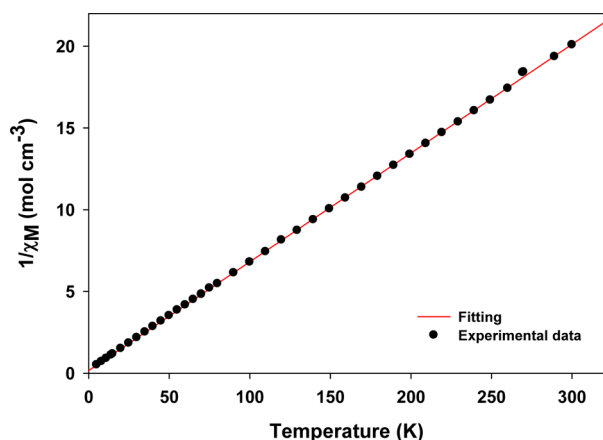

Figure 8. $1/\chi_M$ vs T dependence.

Therefore, only the data above 24 K were considered for the fit. Fitting of the experimental χ_M data led to $J = -4.4(8)$, $J' = -0.3(4)$ cm^{-1}, and $g = 2.00(5)$ (goodness of fit coefficient $R^2 = 0.9992$; Figure 7b). As expected, both couplings are weak, and the coupling between the two distant Ni centers is considerably smaller than the coupling between the two adjacent ones. Although the magnitude of the adjusted J value is considerably lower than the J value obtained from the van Vleck fit, it is still higher than the J' value by an approximate factor of 6, also
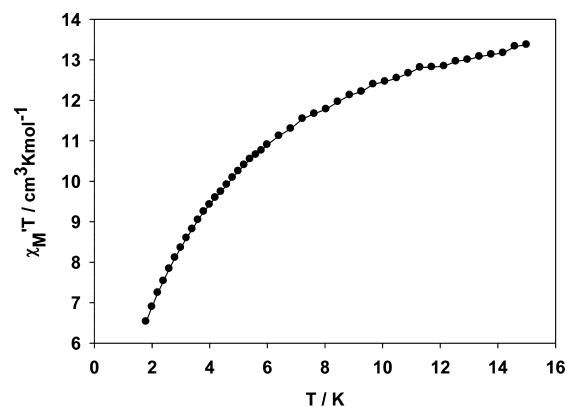

Figure 9. Alternating current $\chi_M'T$ vs T plot.
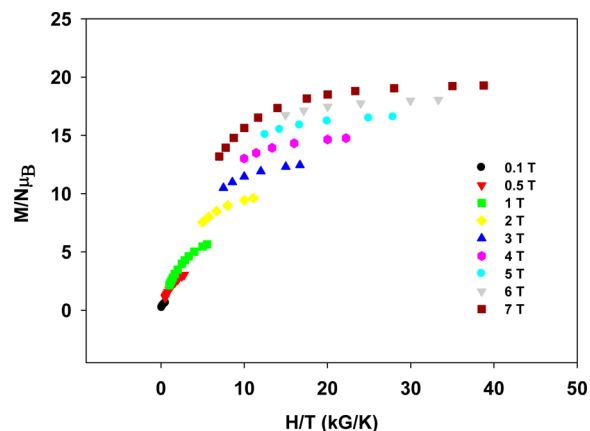
Figure 10. Plot of the reduced magnetization vs field.

Scheme 3. Model of Magnetic Exchange Interactions in 1
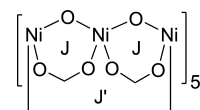
exhibiting weak antiferromagnetic interactions between the adjacent Ni centers. Employing the J and J' values from the van Vleck fit, the energies of the resulting spin states are plotted in Figure 11, indicating a ground state of $S = 1$ for each trinuclear unit. The first and the second excited state are $S = 0$ and $S = 1$, respectively, which is only 7.6 and 16.4 cm^{-1} above the ground

Figure 11. Energy of the states calculated based on the J parameters obtained from a van Vleck fit of the experimental data.

state. The presence of these low-lying excited states is consistent with the conclusions based on the dc, the in-phase ac, and the reduced magnetization analysis. The antiferromagnetic nature of both J and J' provides a potentially spin-frustrated system, but the very weak magnitude of J' vs J and the $S = 1$ g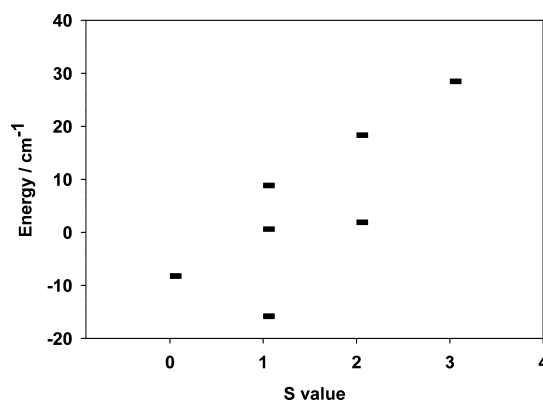round state of the $[Ni_3]$ unit indicate that the magnetic properties are determined by J and the effect of J' is insignificant. Complex **1** is structurally a rare example of an odd-membered ring topology,[32] but magnetically it is best described as five separate $[Ni_3]$ units.

The trinuclear carboxylate−phenoxido-bridged $[Ni_3]$ unit seems to be unprecedented in the reported literature.[33] The most similar systems reported are trimetallic $[Ni_3]$ species with acetate−double phenoxido bridges.[30] The presence of antiferromagnetic coupling can be correlated with the values for the relevant bond angles greater than 90° (Figure 1, bottom).[30]

The ac out-of-phase component for **1** (Figure S4) shows no peak on its temperature dependence determined at 1000 Hz frequency of the oscillating field, which suggests no single-molecule magnet properties.

3. CONCLUSIONS

To sum up, a new wheel-like chiral $[Ni_{15}]$ complex was introduced with a Schiff-base derived from *o*-vanillin and L-glutamic acid acting as a ligand. The presence of the obtained complex molecules was confirmed in solution with methods such as dynamic light scattering and AFM studies on a silicon slide surface. Apart from uniform spherical constructs, the complex superpositioned elements were found in solution and on the AFM image. On the basis of preliminary biological studies low toxicity was confirmed, which are grounds for further, more detailed biological investigations, as only low-cytotoxic substances are candidates for applications such as gene transfer. In particular, the limitation of the preliminary studies was the low solubility in water, which we aim to overcome using nanocarriers, such as particles and liposomes. The host−guest chemistry of the complex itself may also bring new insights into its potential as a model system. Moreover, the specific molecular structure of substance **1** opens promising preconditions to examine its interaction with DNA.[34]

4. EXPERIMENTAL SECTION

4.1. Synthesis and Analytical Data. A 147 mg (1.0 mmol) amount of L-glutamic acid was dissolved in 10 mL of water. Then 408 mg (3.0 mmol) of sodium acetate was dissolved in 10 mL of methanol and added to the solution of L-glutamic acid. A 152 mg (1.0 mmol) portion of *o*-vanillin was dissolved in 5 mL of methanol and added to the stirred L-glutamic acid/sodium acetate solution. The resulting yellow solution was heated to 80 °C and stirred until the solid part was completely dissolved. Then 238 mg (1 mmol) of $NiCl_2 \cdot 6H_2O$ was added to the yellow solution. The solution color changed to green immediately. The solution was stirred for 30 min at 80 °C and was transferred to a 30 mL vial for crystallization by slow evaporation. Green crystals in the form of plates were obtained within 2 weeks in 30% yield.

Elemental analysis for the substance dried under vacuum for several hours, analyzed as $[C_{130.29}H_{160.58}N_{10}Ni_{15}O_{80}]\cdot 4H_2O$: Calcd (found): C 38.17 (38.84), H 4.14 (4.56), N 3.42 (3.22). IR bands (cm^{-1}): 446.9 (m), 484.2 (m), 507.5 (vw), 532.5 (vw), 555.7 (vw), 584.7 (vw), 624.5 (vw), 654.0 (vw), 676.0 (vw), 738.2 (vw), 779.3 (m), 822.6 (vw), 852.4 (vw), 895.0 (vw), 962.5 (w), 1026.4 (vw), 1082.0 (m), 1108.2 (w), 1168.6 (vs), 1213.9 (w), 1240.1 (m), 1292.6 8 (vw), 1349.5 (s), 1386.0 (m), 1420.8 (s), 1441.0 (s), 1456.1 (vs), 1552.7 (vs), 1602.0 (w), 1645.0 (s), 1979.8 (vw), 2035.9 (vw), 2149.3 (vw), 2162.4 (vw), 2323.2 (vw), 2944.5 (vw).

4.2. Physical Measurements. *X-ray Measurement.* X-ray data were collected at 100(2) K on a Bruker Quest D8 diffractometer with a CMOS detector and Mo Kα radiation.[35]

Spectroscopy. IR spectra were collected with the aid of a Bruker Alpha-P infrared-spectrometer equipped with a platinum-ATR with a diamond crystal.

CHN Elemental Analyses. These were carried out on an Elementar Vario Microcube elemental analyzer in CHNS mode.

Energy-Dispersive X-ray spectroscopy (EDX). These measurements were performed on a CamScan 4DV + EDX Noran Instruments Voyager 4.0 with a Pioneer detector.

Thermal Behavior. The TGA diagram for an 11.2 mg sample of **1** was recorded on a Netzsch STA 409 CD device in the temperature range 25−1200 °C at a scanning rate of 5 K/min. The compound slowly released interstitial solvent already starting at room temperature in two steps with mass loss in total attributable to 94 molecules of H_2O or 37 molecules of methanol, which roughly corresponds to the solvent content assessed after application of the SQUEEZE procedure (see refinement details). Further on, a stepwise decomposition is observed (Figure S2), most probably involving release of solvent ligands coordinated to the Ni^{2+} ions in the first place.

Magnetic Measurements. Measurements of the magnetic properties were carried out on a Quantum Design MPMS XL SQUID magnetometer. The powdered microcrystalline sample was restrained in eicosane to prevent torquing. Two kinds of samples were examined: a sample directly after removal from the mother liquor and the sample dried in a vacuum for 2 h. The obtained temperature/field dependences were similar to those in the case of the "wet" sample. However, as clearly degradation of the crystalline phase was observed on drying, the data obtained for a "wet" sample were further evaluated. The molecular mass for the "wet" sample was estimated taking into account the solvent removed by the SQUEEZE procedure during the structure refinement.

Variable-temperature dc magnetic susceptibility measurements were performed in a 0.1 T field in the 5.0−300 K range. The susceptibility data were corrected with respect to the holder and the sample (estimated from Pascal's constants[36]) diamagnetic contribution. Studies for the reduced magnetization plots were carried out at the applied fields of 1000, 5000, 10 000, 20 000, 30 000, 40 000, 50 000, 60 000, and 70 000 Oe.

The temperature-dependent ac susceptibility measurement was performed at 1000 Hz frequency of the oscillating field.

AFM. Substance solution for AFM imaging was prepared in methanol, dropped onto an ultraflat silicon wafer (TED Pella Inc., Redding, CA, USA), and incubated at room temperature for 5 min for the substance to sediment and attach to the surface. To optimize the conditions for the AFM measurement, we have tested the different solutions and concentrations with DLS (see below). The excess methanol was subsequently removed, and the sample area was carefully dried with air. AFM measurements were performed as described previously[37] using NanoWizard (JPK Instruments, Berlin, Germany) in intermittent contact mode with commercially available silicon tips (NSC16 AlBS, Micromasch, Tallinn, Estonia). The image is presented in Figure 3 in the amplitude mode in a 5 × 5 μm frame.

Dynamic Light Scattering. For zeta potential measurements the solutions of substance **1** in 5% methanol/95% water (twice distilled, filtered) were used (see Figure S3). Two concentrations were applied: 2 mg/mL ("diluted") and 6 mg/mL ("concentrated").

The hydrodynamic diameter of the polyplexes was measured in the clear zeta cuvette (Malvern, Herrenberg, Germany) with a Zetasizer Nano ZS (Malvern, Herrenberg, Germany) at 25 °C with 173° backward scattering angle and analyzed using the Smoluchowski model. The number of runs and the attenuator position were adjusted automatically (8−11).

Studies of Stability in Solution by IR Spectrometry. A simple test was also conducted for the solutions of the $[Ni_{15}]$ complex in MeOH and in H_2O/MeOH (95/5). On evaporation of these solutions, a light green powder is obtained, which displays the same IR pattern as recorded for the pure crystalline compound (see Figure S1).

4.3. Studies of Biological Properties. *Details of the Cytotoxicity Assays. Materials.* MTT (3-(4,5-dimethylthiazol-2-yl)-2,5-diphenyltetrazolium bromide) was purchased from Sigma-Aldrich (Taufkirchen, Germany), and the LDH cytotoxicity detection kit was obtained from Roche Diagnostics (Mannheim, Germany).

Preparation of the Test Substance. The test substance was dissolved in methanol; subsequently distilled water was added to obtain the final solution with a 5% methanol content in water. The maximal test substance concentration was set at 1.5 mg/mL and subsequently diluted.

Cell Cultures. B16 mouse melanoma and L929 mouse fibroblasts were cultured in DMEM supplemented with 10% γ-inactivated fetal calf serum (PAA Laboratories, Cölbe, Germany) in a humidified atmosphere with 5% and 7.5% CO_2 at 37 °C, respectively. Subculturing was performed every several days upon 70−80% confluence to new Petri dishes with fresh medium.

I. MTT. The MTT cell proliferation assay[38] measures the cell proliferation rate as a function of metabolic activity in cell mitochondria. When metabolic events coupled with interaction of the test substance within cells lead to apoptosis or necrosis, the reduction in cell viability can be seen. The treated cells that suffer some toxic effect of the test substance have a diminished ability to metabolize the tetrazolium MTT to a substance with an absorption peak at 570 nm. The untreated cells are run as a blank control or a 100% cell viability. All values are related to this control.

B16 and L929 cells were seeded in 96-well plates at a density of 8000 cells/well in a full culture medium (Nunc, Wiesbaden, Germany), then maintained at normal cultivation conditions for 24 h to ensure sufficient cell adherence to the well bottom as reported previously.[39] After treatment with the test substance at different concentrations, starting from 1.5 mg/mL for 4 or 24 h, respectively, the medium was replaced by a serum-free medium containing MTT reagent and incubated again for 4 h. Cell viability was determined by measuring the absorbance of the enzymatically formed formazan at 570 nm with 690 nm background corrections; prior to measurement the cells were lysed in 200 μL of DMSO. The results are presented here as mean values of four replicates with standard deviation.

II. LDH Cytotoxicity Assay. Lactate dehydrogenase (LDH)[40] is a soluble cytosolic enzyme present in most eukaryotic cells and is released into the culture medium upon cell death due to damage of the plasma membrane. The plasma membrane may be damaged due to interactions with a test substance. The increase of the LDH activity in the culture supernatant is proportional to the number of cells with a damaged membrane or lysed cells. As a 100% toxicity control Triton-X can be used, as it is known to effectively lyse the cell membrane. Physiological cell metabolism leads to induction of LDH in the culture medium; at normal conditions untreated cells have up to 10% cellular toxicity assigned to that.

4.4. Details of Structure Refinement. The crystal structure **1** was solved with SHELXS97 and refined with SHELXL97 software.[41] On the basis of systematic absences the $P2_1$ space group type was chosen with absolute configuration consistent with pure enantiomer reagent used in the synthesis, as well as with X-ray diffraction studies. C-bonded H atoms were generated in their calculated positions with $U_{eq} = 1.2/1.5U_{eq}$(parent C atom) for aromatic, methylene/methyl H atoms, respectively. Other H atoms were not found on difference Fourier maps. Four ordered water molecules (O21W−O24W) were localized. Terminal solvent molecules bonded to Ni^{2+} ions were found to be water ligands, except for one site, where occupational disorder presence had to be assumed, with methanol/water components. The corresponding occupancies were refined and then constrained at the refined values (∼0.29 for the methanol ligand; the O atom was assumed to retain its position in both components; a DFIX restraint was used for the C−O bond length). For the N18/N19/N10-containing ligands the AFIX 66 constraint had to be applied to the C18/C19/C10 phenyl rings. For the N18 ligand additional disorder of one −CH$_2$COO moiety had to be assumed, causing difficulties even in localizing the corresponding atoms. The presence of two components was assumed (refined occupancies of 0.57(2)/0.43(2), respectively). For one component the DFIX restraint was used for the carboxyl O···

O distance and a FLAT restraint was applied to the whole moiety. Moreover, the SAME restraint was used to make the geometrical parameters of the disordered moiety components coordinated to Ni^{2+} ions similar to that in the case of the ordered C123-containing moiety, coordinated to Ni4. For the N12/N13/N14 ligands the positions of the C12/C13/C14 aromatic rings were assumed to be disordered in two positions with half-occupancies, with isotropic temperature factors for most displaced atoms. AFIX 66 constraints were used to keep the right geometrical parameters for the corresponding phenyl rings. A combination of SIMU/ISOR/EADP restraints was also applied in some cases. The SQUEEZE procedure[42] had to be applied for the treatment of the remaining heavily disordered solvent molecules in voids between the molecules. In total, three voids were treated, of 7106, 4, and 4 Å^3 volume, containing 1782/4/4 electrons per unit cell, respectively. This should correspond approximately to either 50 methanol or 111 water molecules per asymmetric unit.

On the final difference Fourier map the highest peak of 0.80 e/Å^3 is located at the C88−C128 bond within the disordered ligand moiety, 2.96 Å to Ni12.

CCDC-972059 contains the supplementary crystallographic data for this paper. These data can be obtained free of charge from the Cambridge Crystallographic Data Centre via www.ccdc.cam.ac.uk/data_request/cif.

■ ASSOCIATED CONTENT

Ⓢ Supporting Information

Details of the physical property/stability measurements (magnetic properties, EDX, IR, DLS, TGA, crystallographic tables). This material is available free of charge via the Internet at http://pubs.acs.org.

■ AUTHOR INFORMATION

Corresponding Author
*E-mail: holynska@staff.uni-marburg.de.

Author Contributions
S.M. and M.H. performed syntheses and structural analyses; O.S. and I.L. performed the studies of biological properties/AFM, L.P., M.H., and G.C. performed magnetic measurements and their detailed analysis. All authors cowrote the paper.

Notes
The authors declare no competing financial interest.

■ ACKNOWLEDGMENTS

■ REFERENCES

(1) (a) Holm, R. H.; Kennepohl, P.; Solomon, E. I. *Chem. Rev.* **1996**, *96*, 2239. (b) Lippard, S. J.; Berg, J. M. In *Principles of Bioinorganic Chemistry*; University Science Books: Mill Valley, CA, 1994. (c) Therrien, B.; Süss-Fink, G.; Govindaswamy, P.; Renfrew, A. K.; Dyson, P. J. *Angew. Chem., Int. Ed.* **2008**, *47*, 3773.

(2) (a) Anbu, S.; Kamalraj, S.; Varghese, B.; Muthumary, J.; Kandaswamy, M. *Inorg. Chem.* **2012**, *51*, 5580. (b) Cimerman, Z.; Galic, N.; Bosner, B. *Anal. Chim. Acta* **1997**, *343*, 145.

(3) (a) Halcrow, M. A.; Christou, G. *Chem. Rev.* **1994**, *94*, 2421. (b) Fontecave, M.; Menage, S.; Duboc-Toia, C. *Coord. Chem. Rev.* **1998**, *178*, 1555. (c) Mukhopadhyay, S.; Mal, S. K.; Bhad-uri, S.; Armstrong, W. H. *Chem. Rev.* **2004**, *104*, 3981. (d) Nayak, S.; Nayek, H. P.; Dehnen, S.; Powell, A. K.; Reedijk, J. *Dalton Trans.* **2011**, *40*, 2699.

(4) (a) Bagai, R.; Christou, G. *Chem. Soc. Rev.* **2009**, *38*, 1011. (b) Leuenberger, M. N.; Loss, D. *Nature* **2001**, *410*, 789. (c) Aromi, G.; Brechin, E. K. *Struct. Bonding (Berlin)* **2006**, *122*, 1. (d) Gatteschi,

D.; Sessoli, R. *Angew. Chem., Int. Ed.* **2003**, *42*, 268. (e) Christou, G.; Gatteschi, D.; Hendrickson, D. N.; Sessoli, R. *MRS Bull.* **2000**, *25*, 66.

(5) Kauzmann, W. *Adv. Protein Chem.* **1959**, *14*, 1.

(6) Tanford, C. *Protein Sci.* **1997**, *6*, 1358.

(7) Tanford, C. *The Hydrophobic Effect: Formation of Micelles and Biological Membranes*, 2nd ed.; Wiley, New York, 1980.

(8) Tanford, C. *Science* **1978**, *200*, 1012.

(9) (a) Nelson, D. L.; Cox, M. M. In *Lehninger Principles of Biochemistry*, 4th ed.; Freeman: New York, 2005. (b) Baron, R.; Setny, P.; McCammon, J. A. *J. Am. Chem. Soc.* **2010**, *132*, 12091. (c) Ball, P. *Nature* **2011**, *478*, 467.

(10) Liu, T.; Diemann, E.; Li, H.; Dress, A. W. M.; Müller, A. *Nature* **2003**, *426*, 59.

(11) (a) Thio, Y.; Toh, S. W.; Xue, F.; Vittal, J. J. *Dalton Trans.* **2014**, *43*, 5998. (b) Dearden, A. L.; Parsons, S.; Winpenny, R. E. P. *Angew. Chem., Int. Ed.* **2001**, *40*, 152. (c) Li, J.; Tao, J.; Huang, R.-B.; Zheng, L.-S. *Inorg. Chem.* **2012**, *51*, 5988. (d) Nakajima, T.; Seto, K.; Horikawa, F.; Shimizu, I.; Scheurer, A.; Kure, B.; Kajiwara, T.; Tanase, T.; Mikuriya, M. *Inorg. Chem.* **2012**, *51*, 12503. (e) Brechin, E. K.; Gould, R. O.; Harris, S. G.; Parsons, S.; Winpenny, R. E. P. *J. Am. Chem. Soc.* **1996**, *118*, 11293. (f) Andres, H.; Basler, R.; Blake, A. J.; Cadiou, C.; Chaboussant, G.; Grant, C. M.; Güdel, H.-U.; Murrie, M.; Parsons, S.; Paulsen, C.; Semadini, F.; Villar, V.; Wernsdorfer, W.; Winpenny, R. E. P. *Chem.—Eur. J.* **2002**, *8*, 4867. (g) Cadiou, C.; Murrie, M.; Paulsen, C.; Villar, V.; Wernsdorfer, W.; Winpenny, R. E. P. *Chem. Commun.* **2001**, 2666. (h) Sydora, O. L.; Wolczanski, P. T.; Lobkovsky, E. B.; Rumberger, E.; Hendrickson, D. N. *Chem. Commun.* **2004**, 650. (i) Blake, A. J.; Grant, C. M.; Parsons, S.; Rawson, J. M.; Winpenny, R. E. P. *J. Chem. Soc., Chem. Commun.* **1994**, 2363. (j) Decker, A.; Fenske, D.; Maczek, K. *Angew. Chem., Int. Ed. Engl.* **1996**, *35*, 2863. (k) Zhang, C.; Matsumoto, T.; Samoc, M.; Petrie, S.; Meng, S.; Corkery, T. C.; Stranger, R.; Zhang, J.; Humphrey, M. G.; Tatsumi, K. *Angew. Chem., Int. Ed.* **2010**, *49*, 4209. (l) Zhang, S.; Zhen, L.; Xu, B.; Inglis, R.; Li, K.; Chen, W.; Zhang, Y.; Konidaris, K. F.; Perlepes, S. P.; Brechin, E. K.; Li, Y. *Dalton Trans.* **2010**, *39*, 3563. (m) Angamuthu, R.; Kooijman, H.; Lutz, M.; Spek, A. L.; Bouwman, E. *Dalton Trans.* **2007**, 4641.

(12) (a) Fenske, D.; Ohmer, J. *Angew. Chem., Int. Ed. Engl.* **1987**, *26*, 148. (b) Hong, M.; Huang, Z.; Liu, H. *J. Chem. Soc., Chem. Commun.* **1990**, 1210. (c) Berti, E.; Cecconi, F.; Ghilardi, C. A.; Midollini, S.; Orlandini, A. *Inorg. Chem. Commun.* **1999**, *2*, 146. (d) Albano, V. G.; Demartin, F.; Femoni, C.; Iapalucci, M. C.; Longoni, G.; Monari, M.; Zanello, P. *J. Organomet. Chem.* **2000**, *593–594*, 325.

(13) (a) Bembi, R.; Tandon, O. P. *J. Inorg. Nucl. Chem.* **1981**, *43*, 565. (b) Malik, W. U.; Bembi, R.; Bhargava, P. P.; Sushila; Tandon, O. P. *J. Ind. Chem. Soc.* **1980**, *57*, 455.

(14) Andreeff, M.; Goodrich, D. W.; Pardee, A. B. In *Holland-Frei Cancer Medicine*, 5th ed.; BC Decker: Hamilton (ON), 2000.

(15) Pelin, M.; Sosa, S.; Della Loggia, R.; Poli, M.; Tubaro, A.; Decorti, G.; Florio, C. *Food Chem. Toxicol.* **2012**, *50*, 206.

(16) Morita, H.; Umeda, M.; Ogawa, H. I. *Mut. Res.* **1991**, *261*, 131.

(17) Afrasiabi, Z.; Sinn, E.; Chen, J.; Ma, Y.; Rheingold, A. L.; Zakharov, L. N.; Rath, N.; Padhye, S. *Inorg. Chim. Acta* **2004**, *357*, 271.

(18) Afrasiabi, Z.; Sinn, E.; Padhye, S.; Dutta, S.; Padhye, S.; Newton, C.; Anson, C. E.; Powell, A. K. *J. Inorg. Biochem.* **2003**, *95*, 306.

(19) Afrasiabi, Z.; Sinn, E.; Lin, W.; Ma, Y.; Campana, C.; Padhye, S. *J. Inorg. Biochem.* **2005**, *99*, 1526.

(20) Liu, Y.-C.; Song, X.-Y.; Chen, Z.-F.; Gu, Y.-Q.; Peng, Y.; Liang, H. *Inorg. Chim. Acta* **2012**, *382*, 52.

(21) Datta, S.; Seth, D. K.; Gangopadhyay, S.; Karmakar, P.; Bhattacharya, S. *Inorg. Chim. Acta* **2012**, *392*, 118.

(22) Prabhakaran, R.; Kalaivani, P.; Huang, R.; Poornima, P.; Vijaya Padma, V.; Dallemer, F.; Natarajan, K. *J. Biol. Inorg. Chem.* **2013**, *18*, 233.

(23) Li, M. X.; Zhang, L. Z.; Zhang, D.; Ji, B. S.; Zhao, J. W. *Eur. J. Med. Chem.* **2011**, *46*, 4383.

(24) Zhong, X.; Yi, J.; Sun, J.; Wei, H.-L.; Liu, W.-S.; Yu, K.-B. *Eur. J. Med. Chem.* **2006**, *41*, 1090.

(25) Matkar, S. S.; Wrischnik, L. A.; Jones, P. R.; Hellmann-Blumberg, U. *Biochem. Biophys. Res. Commun.* **2006**, *343*, 754.

(26) Zhong, X.; Wei, H.-L.; Liu, W.-S.; Wang, D.-Q.; Wang, X. *Bioorg. Med. Chem. Lett.* **2007**, *17*, 3774.

(27) Selvakumaran, N.; Pratheepkumar, A.; Ng, S. W.; Tiekink, E. R. T.; Karvembu, R. *Inorg. Chim. Acta* **2013**, *404*, 82.

(28) Alexiou, M.; Tsivikas, I.; Dendrinou-Samara, C.; Pantazaki, A. A.; Trikalitis, P.; Lalioti, N.; Kyriakidis, D. A.; Kessissoglou, D. P. *J. Inorg. Biochem.* **2003**, *93*, 256.

(29) Dong, X.; Wang, X.; He, Y.; Yu, Z.; Lin, M.; Zhang, C.; Wang, J.; Song, Y.; Zhang, Y.; Liu, Z.; Li, Y.; Guo, Z. *Chem.—Eur. J.* **2010**, *16*, 14181.

(30) Pons-Balagu, A.; Piligkos, S.; Teat, S. J.; Sanchez Costa, J.; Shiddiq, M.; Hill, S.; Castro, G. R.; Ferrer-Escorihuela, P.; SaÇudo, E. C. *Chem.—Eur. J.* **2013**, *19*, 9064.

(31) (a) Mukherjee, P.; Drew, M. G. B.; Gomez-Garcia, C. J.; Ghosh, A. *Inorg. Chem.* **2009**, *48*, 4817. (b) Lu, J.-W.; Chen, C.-Y.; Kao, M.-C.; Cheng, C.-M.; Wie, H.-H. *J. Mol. Struct.* **2009**, *936*, 228.

(32) (a) Cannon, R. D.; White, R. P. *Prog. Inorg. Chem.* **1988**, *36*, 195. (b) Cage, B.; Cotton, F. A.; Dalal, N. S.; Hillard, E. A.; Rakvin, B.; Ramsey, C. M. *J. Am. Chem. Soc.* **2003**, *125*, 5270.

(33) CCDC ver. 5.34, November 2013.

(34) (a) Atkinson, H.; Chalmers, R. *Genetica* **2010**, *138*, 485. (b) Matulis, D.; Rouzina, I.; Bloomfield, V. A. *J. Mol. Biol.* **2000**, *296*, 1053.

(35) Bruker AXS. *APEX2* v2012.10-0; 2012.

(36) König, E. *Magnetic Properties of Coordination and Organometallic Transition Metal Compounds*; Hellwege, K. H.; Hellwege, A. M., Eds.; Springer: Berlin, 1966; pp 27−29

(37) Samsonova, O.; Glinca, S.; Biela, A.; Pfeiffer, C.; Dayyoub, E.; Sahin, D.; Klebe, G.; Kissel, T. *Acta Biomater.* **2013**, *9*, 4994.

(38) Zheng, M.; Liu, Y.; Samsonova, O.; Endres, T.; Merkel, O.; Kissel, T. *Int. J. Pharm.* **2012**, *1* (427), 80.

(39) Liu, Y.; Samsonova, O.; Sproat, B.; Merkel, O.; Kissel, T. *J. Controlled Release* **2011**, *163*, 262.

(40) Smith, S. M.; Wunder, M. B.; Norris, D. A.; Shellman, Y. G. *PLoS One* **2011**, *6*, e26908.

(41) Sheldrick, G. M. *SHELXTL 5.1*; Bruker AXS Inc.: Madison, WI, USA, 1997.

(42) Spek, A. L. *Acta Crystallogr.* **2009**, *D65*, 148.